JURNAL KIMIA (*JOURNAL OF CHEMISTRY*) 19 (2), JULI 2025 **p-ISSN 1907-9850**
DOI: https://doi.org/10.24843/JCHEM.2025.v19.i02.p14 **e-ISSN 2599-2740**

STRUCTURAL ANALYSIS, OPTICAL AND PHOTOLUMINESCENCE PROPERTIES OF Ti-ACTIVATED Sr_2SnO_4 SYNTHESIZED BY MEANS OF SOLID-STATE REACTION METHOD

M. Mahmud, F. Failamani, B. Prijamboedi*

Division of Inorganic and Physical Chemistry, Faculty of Mathematics and Natural Sciences, Institut Teknologi Bandung, Jalan Ganesha 10, Bandung 40132, Indonesia
****Email: prijamboedi@itb.ac.id***

Article Received on: 23th January 2025 Revised on: 2nd July 2025 Accepted on: 9th July 2025

ABSTRAK

Pada penelitian ini, kami telah mempelajari evolusi struktur, spektrum absorbansi dan fotoluminesensi (PL) dari *solid-solution* $Sr_2Sn_{1-x}Ti_xO_4$ (SSTO-*x*, *x* = 0,00 dan 0,02) yang disintesis dengan menggunakan metode reaksi fasa padat. Analisis difraksi sinar-X mengonfirmasi bahwa semua sampel memiliki pola difraksi dari Sr_2SnO_4. Beberapa penelitian terdahulu telah melaporkan bahwa senyawa Sr_2SnO_4 memiliki tiga polimorf dengan grup ruang *I*4*/mmm*, *Bmab* dan *Pccn*. Analisis difraksi sinar-X lebih lanjut menggunakan metode *refinement Le Bail* dilakukan untuk mengonfirmasi grup ruang yang diadopsi oleh masing-masing sample. Hasil analisis *refinement* menunjukkan bahwa semua sampel memiliki struktur ortorombik dengan grup ruang *Pccn* yang didasarkan pada nilai *Figure-of-Merits* yang lebih rendah untuk grup ruang ini dibandingkan dua grup ruang lainnya. Selain itu, substitusi ion Sn^{4+} oleh Ti^{4+} menyebabkan penurunan parameter kisi a dan b, sementara itu parameter kisi c mengalami peningkatan yang dapat dikaitkan dengan jari-jari ionic Ti^{4+} yang lebih kecil dibandingkan ion Sn^{4+} dengan bilangan koordinasi yang sama. Spektrum reflektansi masing-masing sampel diperoleh dari pengukuran *UV-Vis Diffused reflectance spectrometry.* Puncak absorpsi untuk sampel SSTO-0 teramati pada panjang gelombang 238 nm, sedangkan puncak absorbansi mengalami pergeseran ke 224 nm pada SSTO-0,02. Sementara itu, puncak absorbansi dengan intensitas rendah juga teramati disekitar panjang gelombang 300 nm pada sampel SSTO-0,02. Spektrum fotoluminesensi (PL) dari SSTO-0,02 yang dieksitasi dengan radiasi sinar UV (λ_{ex} = 254 nm) menunjukkan puncak emisi lebar pada rentang 350 nm hingga 550 nm. Berdasarkan hasil analisis ini diketahui bahwa ion Ti^{4+} pada struktur kristal berperan sebagai pusat luminesensi yang menghasilkan emisi biru.

Kata kunci: analisis struktur, *refinement*, absorpsi, energi celah pita, fotoluminesensi

ABSTRACT

In this work, we have studied the structural evolution, absorption, and photoluminescence (PL) spectra of the Sr_2Sn_1-xTi_xO_4 (SSTO-*x*, *x* = 0.00 and 0.02) solid solution synthesized using the solid-state reaction method. The X-ray diffraction analysis confirmed that all samples possess similar diffraction patterns to Sr_2SnO_4. Some studies reported that Sr_2SnO_4 has three polymorphs with the space groups of *I*4*/mmm*, *Bmab*, and *Pccn*. To confirm the structure of each solid solution, we analyzed the X-ray powder diffraction pattern using *the Le Bail* method based on three reported space groups. Refinement analysis confirmed an orthorhombic polymorph with *Pccn* space group in all samples according to *Figure-of-Merits*, which had a lower residual profile (*Rp* and *Rwp*) and *Goodness-of-Fit* ($\chi 2$). The introduction of Ti^{4+} on Sn^{4+}-sites caused the reduction of lattice parameters *a* and *b*. While the lattice parameter *c* became larger, owing to the smaller Ti^{4+} radii compared to the larger Sn^{4+}, with the same coordination number. The reflectance spectra of all samples were collected from a UV-Vis Diffuse reflectance spectrometer. The absorption peak was observed at 238 nm for SSTO-0 and then shifted to 224 nm for SSTO-0.02. Moreover, a new absorption peak was observed at about 300 nm for samples with Ti^{4+} substitution. The photoluminescence (PL) spectrum of SSTO-0.02 excited by UV radiation (λ_{ex} = 254 nm) showed a broad emission peak in the range of 350 − 550 nm. These results showed that the Ti^{4+} ion is responsible for the luminescence center of blue emission in this material.

Keywords: structural analysis, refinement, optical absorption, bandgap energy, photoluminescence

INTRODUCTION

Blue photoluminescent materials are widely used in the fabrication of white-light emission diodes (WLEDs), which are extensively employed in solid-state lighting. However, blue-emitting materials with a high efficiency are considered rare in photoluminescence applications. Gallium nitride (GaN) has been one of the most reported materials for blue photoluminescence in solid-state lighting (Gaffuri et al., 2021). However, GaN is often deemed an impractical choice for blue-emitting material due to its complex and costly manufacturing process. As a result, numerous studies have been conducted to identify alternative materials that are not only easier to synthesize but also offer higher efficiency.

Strontium orthostannate (Sr_2SnO_4), one of the perovskite-like structure compounds, has been reported as a potential host material for various photoluminescence materials (Fang et al., 2018; Kamimura et al., 2012; Kumar et al., 2021). It offers high stability with relatively easy and low cost in the manufacturing process. Previous studies have indicated that Sr_2SnO_4 can exist in three polymorphs: orthorhombic *Pccn*, orthorhombic *Bmab*, and tetragonal *I4/mmm*, with each structure occurring at different temperatures. The higher-symmetry tetragonal *I4/mmm* was reported to exist at temperature above 573 K, while the lower-symmetry orthorhombic *Bmab* and *Pccn* were found at temperature above 423 K and 300 K, respectively (Fu et al., 2004).

Sr_2SnO_4 compound itself does not exhibit any photoluminescence properties. In order to generate photoluminescence emissions, Sr_2SnO_4 is often doped with other elements, typically rare-earth metals or transition ones. Rare earth doping in this material results in various emission spectra depending on the element doped to the structure. For example, Sm^{3+}-doped Sr_2SnO_4 emitted bright reddish-orange color, Tb-Mg co-doped Sr_2SnO_4 emitted bright green color, while Eu-Ti co-doping in Sr_2SnO_4 results in magenta emission (Kamimura et al., 2012; Ueda et al., 2006). However, the utilization of rare-earth elements as activators for photoluminescence materials is limited due to their low abundance and the high costs of the extraction processes. Interestingly, Ti-doped Sr_2SnO_4 has been reported to emit bright blue luminescence (Yamashita and Ueda, 2007) but the effect of Ti substitution on the structure of Sr_2SnO_4 has not been reported in the literature yet.

In this study, Sr_2SnO_4 and Ti-doped Sr_2SnO_4 samples are synthesized by means of a conventional solid-state reaction method. The diffraction pattern of both samples measured using x-ray powder diffraction method are analysed to investigate the most possible structure of both samples among the three polymorphs. Furthermore, the refinement analysis is employed to those diffraction patterns, to study the effect of Ti doping on the structural parameters. The optical reflectance spectra are also recorded to study the effect of the introduction of small amount of Ti ion at Sn-sites on the absorption characteristic. Further analysis is performed to estimate the bandgap energy using Kubelka-Munk analysis. Lastly, photoluminescence analysis is performed to investigate the effect of Ti ion doping in Sr_2SnO_4 on the photoluminescence emission and excitation spectrum and to understand the photoluminescence mechanism in Ti-doped Sr_2SnO_4.

EXPERIMENTAL PROCEDURES

$Sr_2Sn_{1-x}Ti_xO_4$ (SSTO-*x*), where *x* is 0 and 0.02 mol, is synthesized using a conventional solid-state reaction method. High purity $SrCO_3$ (Aldrich, 99.9%), SnO_2 (Aldrich, 99.9%) and TiO_2 (Aldrich, 99.8%) are used as precursors. Those precursors are weighted with respect to the target formula SSTO-0 and SSTO-0.02. All precursors are mixed and grounded for 6 hours. The mixture is pre-fired for 12 hours at 1000 °C to eliminate CO_2 from the carbonate precursor. The pre-heated powder is re-ground for another 6 hours and then it is pressed to a cylindrical pellet. The pellet is heated for 12 hours at 1200 °C. For the characterization purpose, the as-synthesized pellets are ground to obtain a fine powder.

X-ray powder diffractometer (XRPD, Rigaku xtaLAB mini II) is utilized to collect the diffractograms of both SSTO-0 and SSTO-0.02 samples. Both pellets are ground to obtain a fine powder and its diffraction angle is collected from 10° to 90°. Further diffraction analysis is carried out using *Le Bail* refinement method (RIETICA software) to confirm the space group possessed by both SSTO-0 and SSTO-0.02. The

standard models used in this analysis is based on three different space groups, i.e. *Pccn*, *Bmab*, and *I4/mmm*, reported by Fu *et. al.* (2007). In addition, the lattice parameters change due to the increase in Ti^{4+} content is also obtained from this analysis. In order to analyze the effect of Ti doping on optical properties, especially the reflection spectrum and bandgap energy, the reflection spectra are measured using UV-Visible Diffused Reflectance Spectrophotometer (DRS, Thermo-Scientific Evolution). The bandgap energy is estimated using Kubelka-Munk function (F[R]) while the energy for direct allowed and indirect allowed transitions is plotted as a function of $(F[R]hv)^2$ and $(F[R]hv)^{1/2}$ vs photon energy (hv), respectively. Meanwhile, the photoluminescence emission (PL) and excitation (PLE) spectra are characterized using Spectrofluorometer (Shimadzu RF-5301). The excitation wavelength used for collecting PL spectra is 254 nm, while the emission wavelength for PLE is fixed at 430 nm.

RESULTS AND DISCUSSIONS

Diffractogram of both SSTO-0 and SSTO-0.02 are shown in Fig. 1a. All samples exhibit a similar diffraction pattern compared to three diffraction models, indicating Sr_2SnO_4 and Ti-doped Sr_2SnO_4 have been successfully synthesized by following the conventional solid-state method. The effect of Ti-doped on crystal structure is analyzed by comparing the most intense reflection peak around 29-33°. Fig. 1.b depicts the magnification of the two main diffraction peaks. The diffractogram shows a noticeable shift on diffraction peaks to a higher diffraction angle with Ti doping on crystal structure. It might indicate the change in cell volume due to the introduction of Ti^{4+} at Sn^{4+}-sites in crystal structure of Sr_2SnO_4. The change in cell volume, then, leads to the change in atomic distance resulting in the change in interplanar spacing.

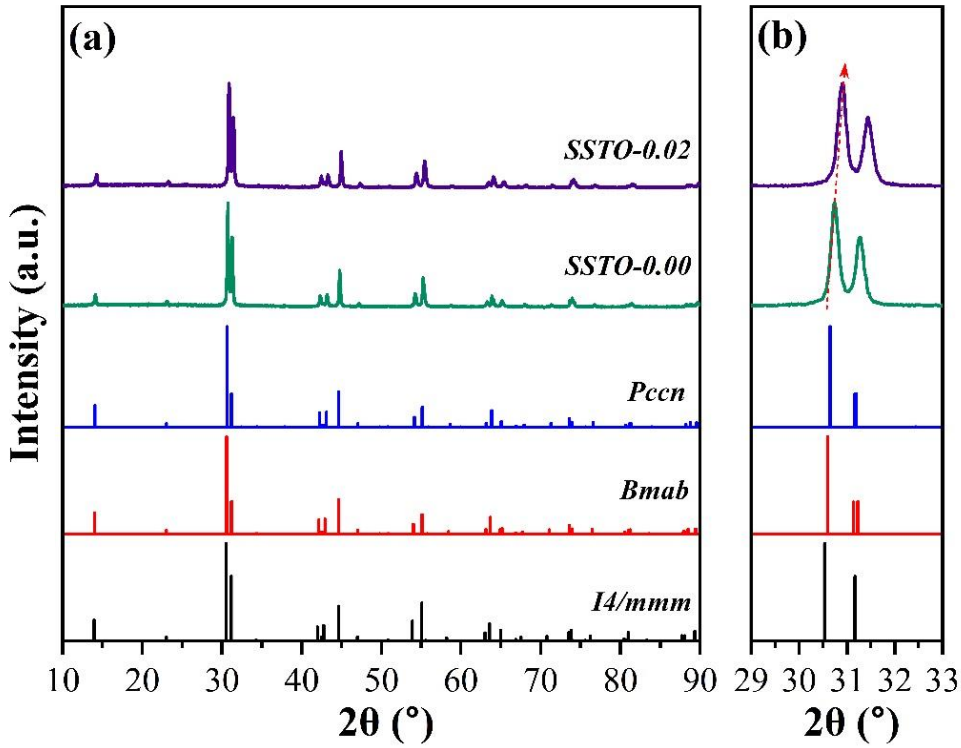

Figure 1. (a) X-ray diffraction pattern of SSTO-0 and SSTO-0.02 compared to three diffraction model reported for Sr_2SnO_4, and (b) the magnification at the most intense diffraction peak.

Furthermore, from Fig. 1, we notice no prominent difference among three reported standard models for Sr_2SnO_4, hence we cannot determine the possible structure that possessed by both sample at room temperature only by comparing the diffraction pattern among three different structures.

In order to determine the most possible crystal structure of SSTO-0 and SSTO-0.02, both diffractogram samples are refined using *Le Bail* method. The crystallographic information such as lattice parameter of *Pccn*, *Bmab* and *I4/mmm* used as standard model was reported in the previous study (Fu *et al*., 2004). The refinement plot of SSTO-0 is shown in Fig 2.a. The diffraction pattern of SSTO-0 matches with all calculated diffraction models. There is no significant difference in the refinement plots among all three structural models. The only observable difference is the peak that appears at about 50°, see inset of Fig. 2.a, which only detected as a reflection plane in both orthorhombic *Pccn* and *Bmab* structure, but do not appear as a Bragg reflection of tetragonal *I4/mmm* structure. This reflection in both orthorhombic structures is indicated by the blue marker. A similar result is also observed for SSTO-0.02 sample.

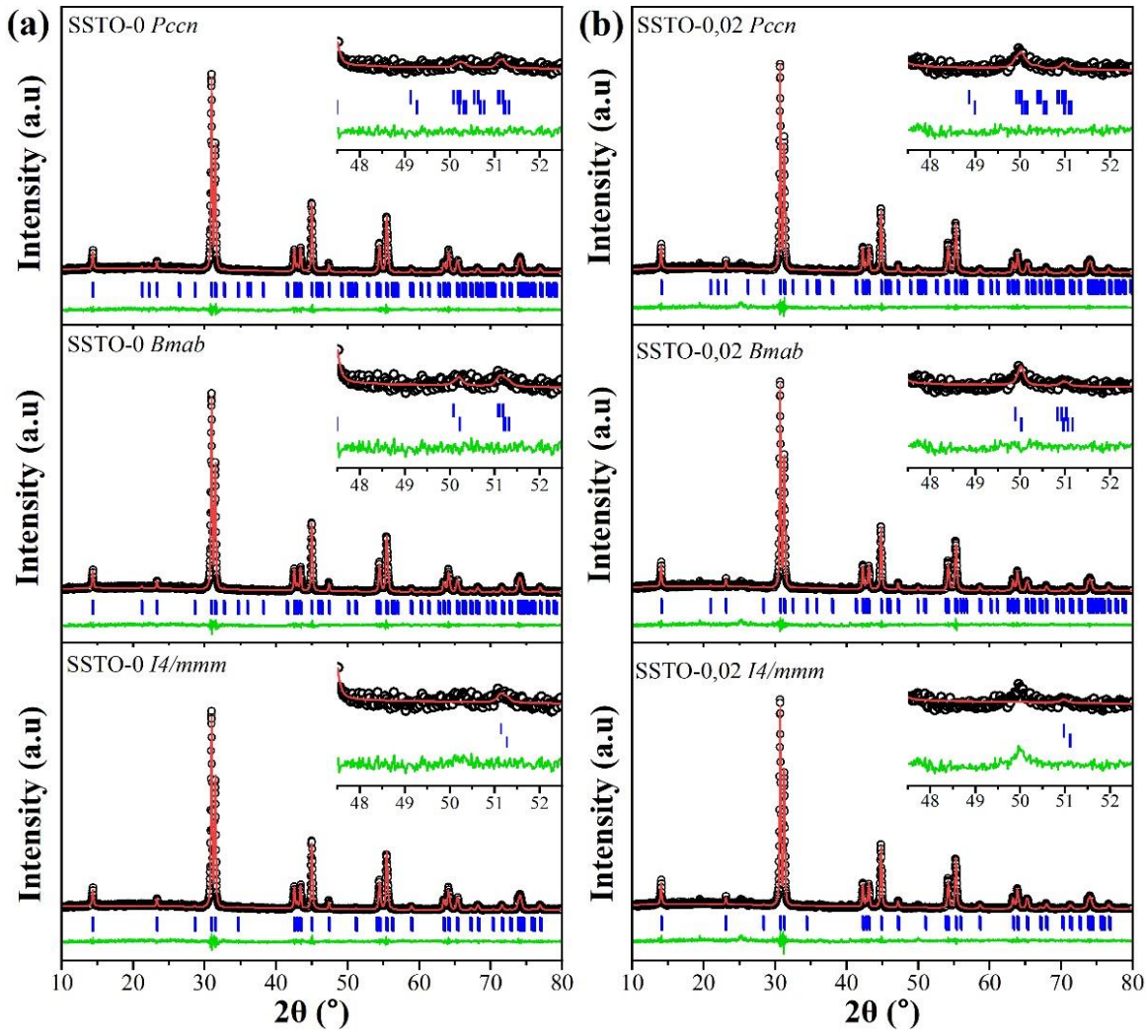

Figure 2. The refinement plot of (a) SSTO-0 and (b) SSTO-0.02 sample. The inset in each individual plot is the magnification of diffraction pattern from 45.5-55°.

Fig 2.b shows the refinement plot of SSTO-0.02 refined with three polymorphs. The observed diffraction data of SSTO-0.02 exhibits good matching with all calculated diffraction models. However, similar result with SSTO-0, the small peak observed around 50° is only detected as the reflection plane for both orthorhombic *Pccn* and *Bmab* structure. Therefore, from the above analysis, we can assume that SSTO-0 and SSTO-0.02 possess an orthorhombic structure. Besides, further structural analysis could also be confirmed by comparing *Figure-of-Merits* (*FoM*), i.e. R_p, R_{wp} and *Goodness-of-Fit* (χ^2), of the individual refinement result. The smaller the value of *FoM*, the greater the possibility of its structural model is possessed by the sample.

Table 1 shows the *FoM* value for SSTO-0 and SSTO-0.02 as results of refinement calculation. Both refined diffraction samples with orthorhombic *Pccn* structure have smaller *FoM* compared to orthorhombic *Bmab* and tetragonal *I4/mmm*. Even though *Pccn* has smaller *FoM*, however, the *FoM* difference among those structures is quite small. Moreover, it is also confirmed by the very similar diffraction pattern of all structures owing to the lowering symmetry of *I4/mmm* to *Pccn* caused by the SnO_6 octahedral tilting. Then, from the above analyses, it could be safe to suggest that SSTO-0 and SSTO-0.02 could possibly adopt the orthorhombic *Pccn* structure.

Table 1. *Figure-of-Merits* (*FoMs*) parameters as the results of refinement analysis for SSTO-0 and SSTO-0.02

Figure-of-Merits (FoMs)	SSTO-0			SSTO-0.02		
Space Group	*Pccn*	*Bmab*	*I4/mmm*	*Pccn*	*Bmab*	*I4/mmm*
R_p (%)	9.36	9.41	10.23	9.22	9.22	9..74
R_{wp} (%)	13.21	13.30	13.97	12.98	13.11	13.76
χ^2	1.29	1.31	1.45	1.35	1.38	1.52

Table 2. Lattice parameters result from the refinement analysis of SSTO-0 and SSTO-0.02

Sampel	SSTO-0	SSTO-0.02	Parameter Change (Δ)
Space Group	*Pccn*	*Pccn*	
Structure	Orthorhombic	Orthorhombic	
Z	4	4	-
a (Å)	5.7263(3)	5.7168(3)	− 0,0095
b (Å)	5.7378(3)	5.7250(4)	– 0.0128
c (Å)	12.587(0)	12.593(1)	+ 0.0060
V (Å^3)	413.57(3)	412.15(4)	– 1.4200
R_p (%)	9.36	9.22	-
R_{wp} (%)	13.21	12.98	-
χ^2	1.29	1.35	-

Table 2 displays the lattice parameters of refined diffraction pattern for SSTO-0 and SSTO-0.02. The effect of Ti^{4+} doping on Sn^{4+} sites is reflected by the change of lattice parameters. The lattice parameters *a* and *b* tend to decrease with Ti^{4+} substitution, while lattice parameter *c* increases. It leads to the shrinking of cell volume. The change in lattice parameter by Ti^{4+} doping could be described by the different ionic radii of Sn^{4+} and Ti^{4+} which occupy B-sites of A_2BO_4 formula. Sn^{4+} (0.69 Å) with six-coordination number has larger ionic radii than that of Ti^{4+} (0.605 Å) with same coordination number (Shannon, 1976). When the smaller ion substitutes the larger ion in its crystal sites, it tends to reduce the octahedral BO_6 cavity followed by the decreasing cell volume. This result is in line with the shifting in diffraction peak to higher angle.

The optical reflectance spectra of SSTO-0 and SSTO-0.02 samples are depicted in Fig. 3. The reflectance spectrum of SSTO-0 sample displays a strong absorption peak at 238 nm, along with two smaller peaks centered at 386 nm and 507 nm. The substitution of Sn^{4+} by Ti^{4+} in SSTO-0.02 shifts the absorption peak of the sample to shorter wavelength, around 224 nm, while the position of the two smaller peaks remains unchanged. Additionally, another small absorption peak appears at 300 nm after doping of Ti in SSTO-0.02 structure.

The appearance of the small absorption peak at SSTO-0.02 may be attributed to the formation of Ti-related states. The shift in absorption edge with Ti doping in SSTO-0.02 suggests a change in bandgap energy. The bandgap energy for direct transition and indirect transition are estimated using Kubelka-Munk function, $(F[R]hv)^2$ and $(F[R]hv)^{1/2}$, respectively, as a function of photon energy (hv).

Fig. 4 exhibits the Tauc plot of SSTO-0 and SSTO-0.02 for direct transition and indirect transition. The direct and indirect energy are obtained by extrapolating the linear portion of the steep region of the individual spectra. The direct bandgap energy increases (see Fig. 4.a) from 4.65 eV for SSTO-0 to 5.10 eV for SSTO-0.02. Similarly, the indirect bandgap also increases from 4.10 eV for SSTO-0 and 4.80 eV with incorporation of Ti in SSTO-0.02. The direct and indirect bandgap energy for SSTO-0 is in line with our previous study (Prijamboedi et al., 2015). This result is consistent with the blue shift of absorption edge in SSTO-0.02 indicating higher energy requirement to achieve an electronic transition from the valence band to the conduction band.

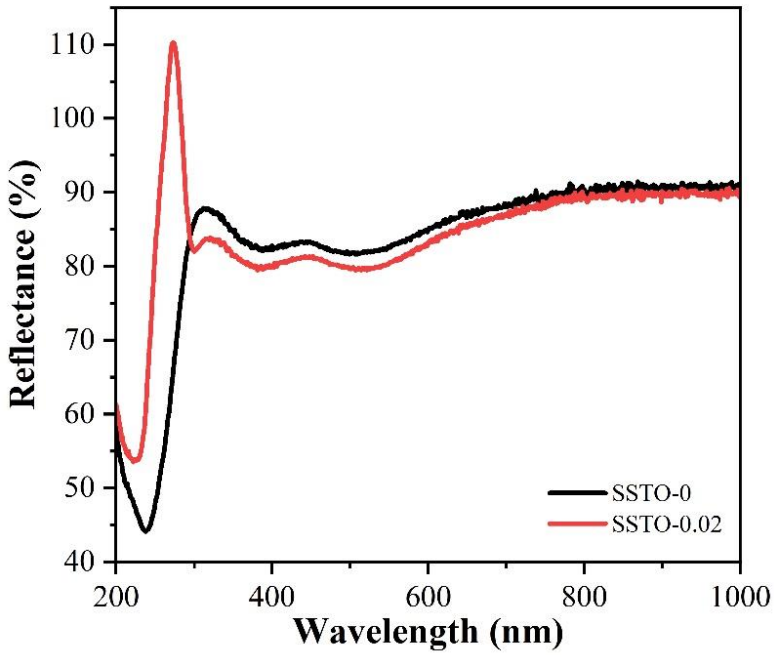

Figure 3. Reflectance spectra of SSTO-0 and SSTO-0.02

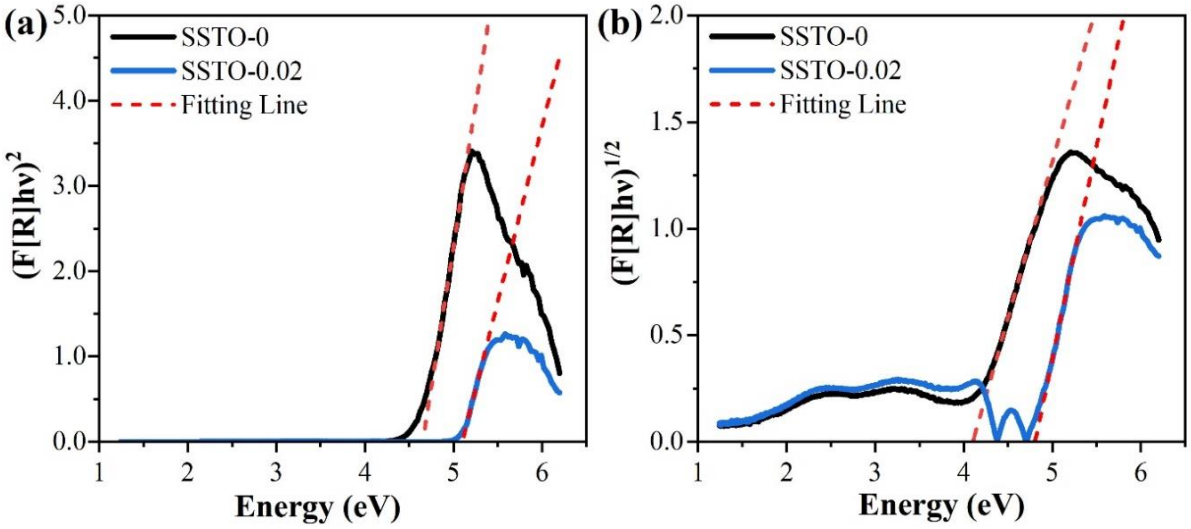

Figure 4. A Tauc plot for (a) direct transition and (b) indirect transition of SSTO-0 and SSTO-0.02

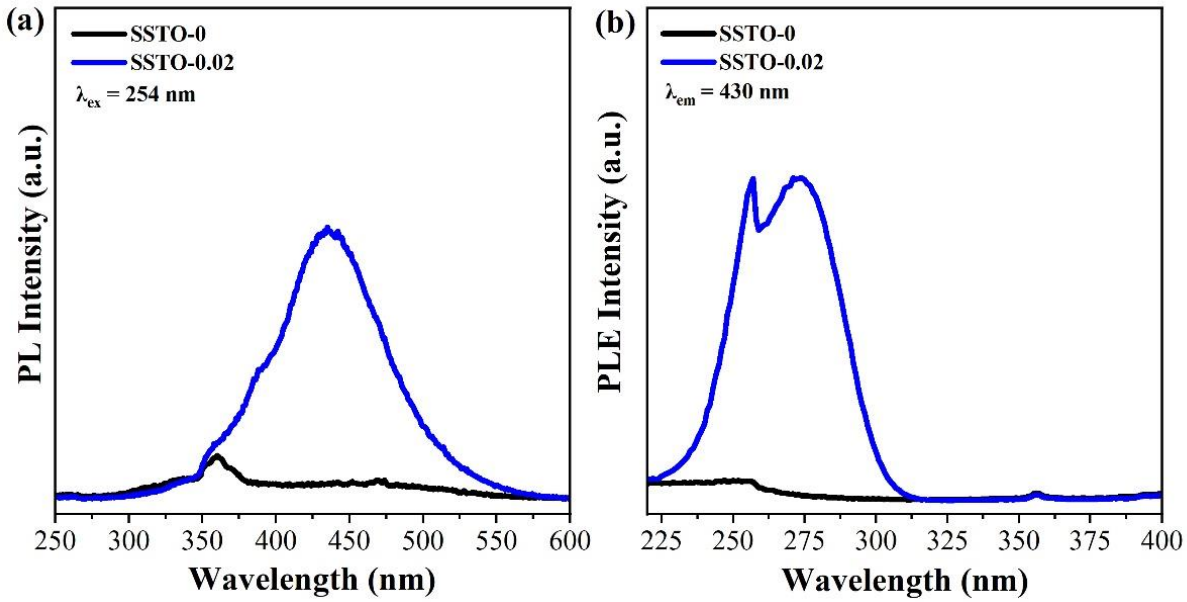

Figure 5. (a) Photoluminescence emission (PL) and (b) Photoluminescence excitation (PLE) spectra of SSTO-0 and SSTO-0.02

The photoluminescence (PL) and photo-luminescence excitation (PLE) spectra for SSTO-0 and SSTO-0.02 are shown in Fig. 5. The PL spectrum of SSTO-0 (Fig. 5.a) reveals a small peak around 360 nm when excited under 254 nm light, which is attributed to a characteristic feature of the host material. In contrast, SSTO-0.02 exhibits a strong emission peak at 435 nm, which in line with the previous study (Yamashita and Ueda, 2007). This blue emission is relatively broad, with a small hump appearing around 393 nm, suggesting that the broad blue emission is composed of several smaller peaks. Deconvolution analysis using Gaussian fitting function is employed to dissociate any signals in the PL emission spectrum of SSTO-0.02. Inset of Figure 5.a shows deconvolution result of SSTO-0.02, where at least three signals has been identified composing SSTO-0.02 spectrum. One of them, about 356 nm, is

observed as similar signal in host material, while two signals at lower energy, about 379 nm and 437 nm, can only be observed at Ti^{4+}-doped sample. Fig. 5.b presents the PLE spectra for both samples with fixed emission wavelength at 430 nm. The SSTO-0.02 sample shows a prominent excitation peak centered at 273 nm, which is absent in SSTO-0. This analysis indicates that titanium (Ti) doping in the host material enhances blue photoluminescence properties in Sr_2SnO_4. The presence of blue luminescence properties in Ti-doped SSTO can be described by the formation of mid-states between valence-band and conduction-band due to the introduction of Ti ions into the lattice. Those mid-states are probably formed by 3d-orbitals of Ti^{4+} ion which have lower energy level compared to 5s-orbital of Sn^{4+} composing the conduction band.

CONCLUSIONS

In conclusion, the synthesized SSTO-0 and SSTO-0.02 diffractograms have good agreement with three structural models reported in previous study. Structural analysis using Le Bail refinement method reveals that both SSTO-0 and SSTO-0.02 possess an orthorhombic *Pccn* structure compared to *Bmab* and tetragonal *I4/mmm*. Ti doping in SSTO-0.02 reduces the cell volume of SSTO-0 due to the substitution of larger Sn^{4+} with smaller Ti^{4+} at the crystal sites. The reflectance spectrum of SSTO-0 sample shows a strong absorption peak at 238 nm, which shifts to a shorter wavelength of 224 nm upon the incorporation of Ti ion in SSTO-0.02. The blue shift in absorption edge indicates the change in bandgap energy with Ti doping in host sample. Kubelka-Munk analysis from DRS data shows that both direct transition and indirect transition energies for electronic transition increase with the introduction of Ti ion into the crystal site. It implies a modification in the electronic structure of host material with Ti doping into the crystal structure. A strong blue emission spectrum is observed in PL spectra of SSTO-0.02 sample which did not appear in SSTO-0 spectrum. Similarly, an intense peak centered at 273 nm in PLE spectra observed only for SSTO-0.02. These results indicate that Ti ion acts as activator for the blue emission center in SSTO-0.02. Therefore, this study suggests that the Ti-doped Sr_2SnO_4 has potential application as a blue photoluminescent material for lighting devices.

REFERENCES

Fang, H., Qiu, G., Wang, X., Li, Y., and Yao, X. 2018. Trap modification and mechanoluminescence improvement by Si substitution for Sn in $Sr_2SnO_4:Sm^{3+}$ ceramics. *Journal of Advanced Dielectrics*. 8(3): 1–6. https://doi.org/10.1142/S2010135X18500169

Fu, W. T., Visser, D., Knight, K. S., and Ijdo, D. J. W. 2004. Neutron powder diffraction study of phase transitions in Sr_2SnO_4. *Journal of Solid State Chemistry*. 177(11): 4081–4086. https://doi.org/10.1016/j.jssc.2004.08.023

Gaffuri, P., Stolyarova, E., Llerena, D., Appert, E., Consonni, M., Robin, S., and Consonni, V. 2021. Potential substitutes for critical materials in white LEDs: Technological challenges and market opportunities. *Renewable and Sustainable Energy Reviews*. 143(March): 110869. https://doi.org/10.1016/j.rser.2021.110869

Kamimura, S., Yamada, H., and Xu, C. N. 2012. Strong reddish-orange light emission from stress-activated $Sr_{n+1}Sn_nO_{3n+1}:Sm^{3+}$ ($n = 1, 2, \infty$) with perovskite-related structures. *Applied Physics Letters*. 101(9): 2–6. https://doi.org/10.1063/1.4749807

Kumar, U., Upadhyay, S., and Alvi, P. A. 2021. Study of reaction mechanism, structural, optical and oxygen vacancy-controlled luminescence properties of Eu-modified Sr_2SnO_4 Ruddlesden popper oxide. *Physica B: Condensed Matter*. 604(October 2020): 412708. https://doi.org/10.1016/j.physb.2020.412708

Prijamboedi, B., Umar, S., and Failamani, F. 2015. Electronic structure and optical properties of Sr_2SnO_4 studied with FP-LAPW method in density functional theory. *THE 5TH ASIAN PHYSICS*

SYMPOSIUM. 030001. 030001. https://doi.org/10.1063/1.4917090

Shannon, R. D. 1976. Revised effective ionic radii and systematic studies of interatomic distances in halides and chalcogenides. *Acta Crystallographica Section A*. 32(5): 751–767. https://doi.org/10.1107/S0567739476001551

Ueda, K., Yamashita, T., Nakayashiki, K., Goto, K., Maeda, T., Furui, K., Ozaki, K., Karachi, Y., Nakamura, S., Fujisawa, M., and Miyazaki, T. 2006. Green, orange, and magenta luminescence in strontium stannates with perovskite-related structures. *Japanese Journal of Applied Physics, Part 1: Regular Papers and Short Notes and Review Papers*. 45(9A): 6981–6983. https://doi.org/10.1143/JJAP.45.6981

Yamashita, T., and Ueda, K. 2007. Blue photoluminescence in Ti-doped alkaline-earth stannates. *Journal of Solid State Chemistry*. 180(4): 1410–1413. https://doi.org/10.1016/j.jssc.2007.02.009